

MEMS Tunable Silicon Fabry-Perot Cavity

Jonathan Masson, Fatou Binetou Koné, Yves-Alain Peter

École Polytechnique de Montréal, Engineering Physics Department
Montréal (Québec) H3C 3A7, CANADA
yves-alain.peter@polymtl.ca

ABSTRACT

In this paper we present an innovative tunable Fabry-Perot cavity micromachined in silicon. A short summary of the theoretical background of these filters is presented, followed by technical requirements for the design of the dielectric mirror composing the Fabry-Perot cavity and the cavity itself. Simulations and experimental data are demonstrated to be in good agreement. An in plane design is used to allow easy fiber alignment. The Fabry-Perot is tuned by an electrostatic comb drive actuator supported by a set of four springs to achieve a uniform modulation of the air gap of the filter. Only 15.4 V are required to tune the Fabry-Perot over 73nm bandwidth (covering more than the whole C-band) with a FWHM varying from 6 to 10nm. Transmission losses are -11dB.

Keywords: MEMs, grating, Fabry-Perot, Bragg, DRIE

1. INTRODUCTION

One dimensional silicon photonic crystals are of great interest for several optical applications. They are made of alternate layers of air and micro machined silicon. They can be actuated to provide tuning of their optical properties and they are fabricated by conventional silicon machining processes. Several designs have been proposed but none of them provide fast and wide tuning range, easy fabrication process, low losses and passive fiber alignment¹⁻⁴. In this paper, we report the fabrication of silicon tunable Fabry-Perot (FP) resonators made of two Bragg reflectors as the mirrors of the FP cavity. Tuning the air gap between the mirrors is made possible with the use of electrostatic comb drive actuators. High aspect ratio etching of silicon enables the fabrication of small size features of the filter at the same time as optical fiber grooves. In plane design allows an easy way for passive fiber alignment.

Such filters have applications in telecommunication, bio-sensing, and tunable lasers⁵. In fact, fiber lasers can be tuned over a large bandwidth as Erbium gain, for example, spans over the C and L bands. Inserting a tunable filter inside the fiber laser cavity makes possible a high power tunable laser suitable for the replacement of many laser sources in telecommunication systems.

In the next sections, we will first summarize the basic theory for designing such filters by studying the optical behavior of Bragg gratings and of Fabry-Perot cavities. In the second part of the paper, we will detail the fabrication process and present fabricated devices characterized optically and electrostatically.

2. THEORY

We use the transfer matrix method to simulate the reflected and transmitted light of wavelength λ across the FP filter⁶. Each layer of silicon and air has its own corresponding characteristic matrix. Let's first consider the Bragg reflectors. We have the following relation between the wavelength and the thickness of each layer:

$$\Lambda = \frac{N\lambda}{4n}, \quad (1)$$

with $n_{Si}=3.45$ and $n_{air}=1$ at a wavelength $\lambda=1550\text{nm}$. At the first order ($N=1$), we have a silicon thickness of $\Lambda_{Si}=112\text{nm}$ and an air of $\Lambda_{air}=388\text{nm}$. However, we can have the dimensions be a multiple of higher order $N=(2m+1)\Lambda_{Si}$, where m is an integer. We would like the reflectors to be of a wide bandwidth to be used as the mirrors of the FP. A wide reflectance bandwidth of the Bragg mirrors will provide a wide tuning range for the FP. The transmission peak of the FP filter will occur within the reflection bandwidth of the mirrors. The orders of the air and silicon layers are the key elements to achieve the wide bandwidth objective. Figure 1 shows the relationship between the silicon walls order and the reflection peak bandwidth of one Bragg reflector. As the order of the walls is decreased, the reflection peak gets larger. The first order is barely visible since it is almost a straight line at the reflectance value of 1.

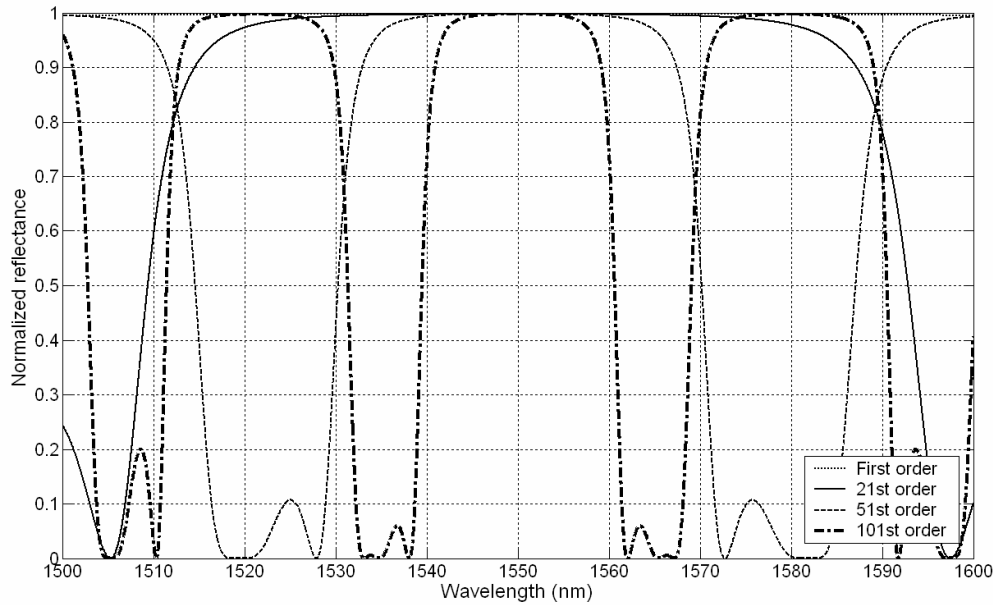


Fig. 1. Normalized reflectance versus wavelength for a three layer grating with four different orders: 1st, 21st, 51st and 101st.

To make a FP cavity, we use two Bragg reflectors separated by an air gap of thickness

$$\Lambda_{FP} = \frac{m\lambda}{2},$$

where m is the order of the air gap of the filter. On figure 2, one can see that higher silicon or air order improves the finesse of the filter, but decreases the stopband, thus limiting the tuning range. A filter with an order around 23rd, seems to be a good compromise between tuning range, finesse, and the size of the walls for ease of fabrication. The number of walls of the Bragg reflectors has an impact on the reflectivity of the Bragg reflector: the higher the number of walls, the higher the reflection and thus a better finesse of the FP cavity. But in practice, since the fabrication process generates deviations on the geometry of the walls, increasing the number of walls will also increase the losses. In fact, the walls are not perfectly vertical due to the deep etching process. Adding more walls will increase losses since light experience multiple reflections on each layer of the grating. We found experimentally that the optimal number of walls is three.

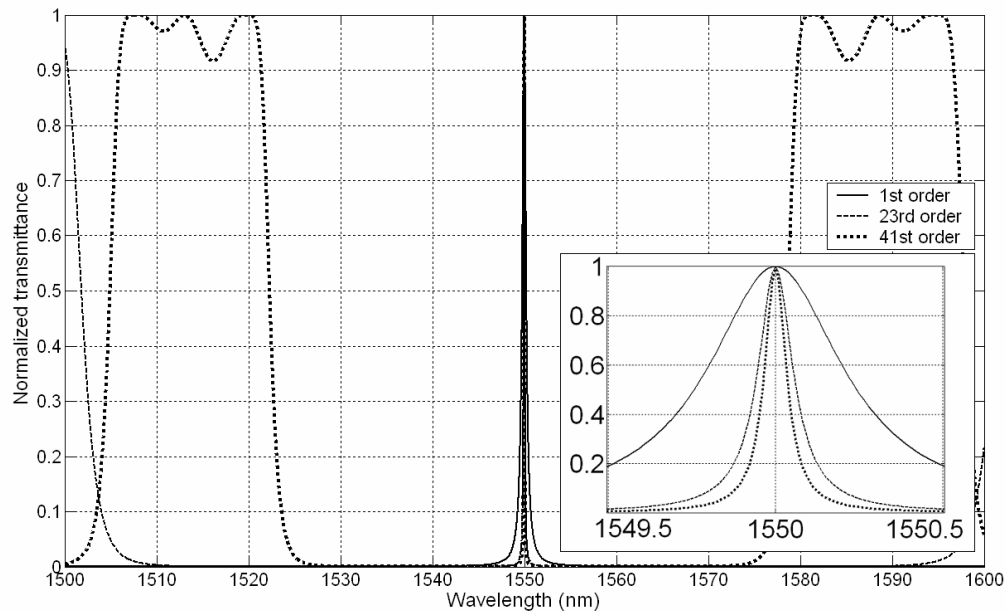


Fig. 2. Normalized transmittance versus wavelength of a Fabry-Perot cavity with two three-layers gratings as reflectors and a gap of λ ($m=2$). Inset: close up view of the peaks for three different orders of the gratings: 1st, 23rd and 41st.

3. FABRICATION

The devices are fabricated by silicon micromachining. We fabricate the Fabry Perot and the optical fiber grooves in one single step of deep reactive ion etching (DRIE) on a 70 μm thick silicon on insulator (SOI) wafer. The process flow is shown on figure 3. (a) We start with 70 μm thick device layer silicon on insulator (SOI) wafer. (b) A 4 μm thick layer of SPR220 3.0 photoresist is spun. A thick masking layer is needed for the 70 μm DRIE step. Figure 3. (c) shows the inductive coupled plasma (ICP) DRIE step. Verticality of the etched structures is of prime importance in order to lower the optical losses of the devices. Therefore, we use a 450W forward ICP power, and 25W and 10W RF power for the etch step and the passivation step respectively. The etching process is made at a pressure of 15mTorr. The pressure is an important factor in the sidewall profile control. Smoothness of the walls can be improved by adding oxygen during the etch step. (d) The 2 μm buried oxide layer is etched away in liquid HF to release the structures and supercritical CO₂ drying is used to prevent the devices from sticking. Two optical fibers can be placed on each side of the FP cavity. They are passively aligned by the deep silicon square grooves. We use 125 μm diameter single mode fibers (Corning SMF-28e) so the top of the fiber core is 5.4 μm lower than the top of the grating to insure a good coupling with the grating.

Figure 4 is a scanning electron micrograph of a fabricated device. The FP cavity is formed by two Bragg reflectors each of them made of three silicon walls (see inset of Fig. 4). One of the Bragg reflectors can be actuated with an electrostatic comb drive suspended by a set of four springs to provide a uniform modulation of the air gap. Applying a voltage difference between the two electrodes will make the combs move closer to each other reducing the air gap of the FP filter. As mentioned in the previous section, reducing the air gap reduces the filtered wavelength.

The vertical roughness of one silicon wall of a Bragg mirror was measured with an AFM, and is 26.2nm rms. Verticality was estimated on a scanning electron micrograph to be less than 0.5°.

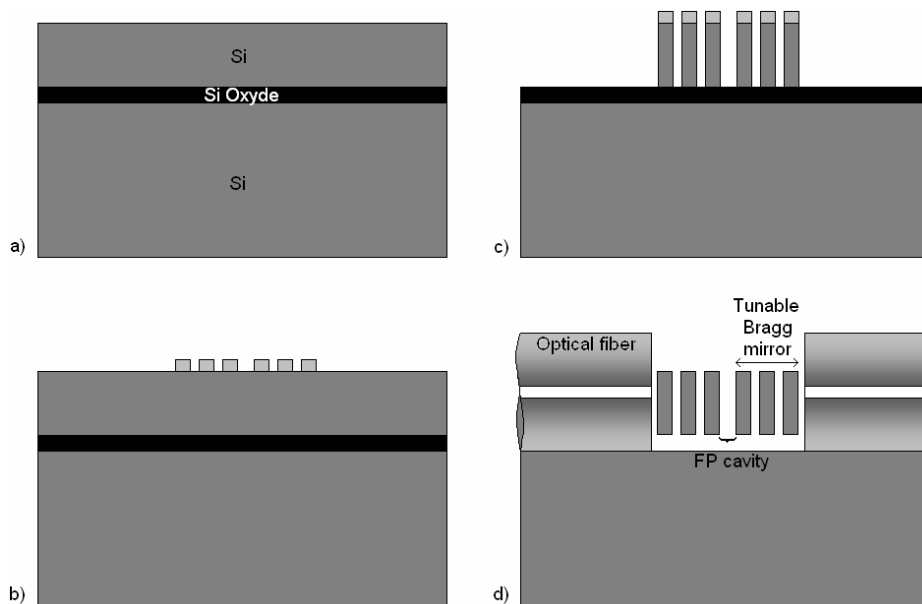


Fig. 3. Microfabrication steps for the tunable FP. (a) A 70 μm thick device layer SOI is used. (b) Photolithography of 4 μm thick resist layer. (c) Vertical etching of the 70 μm device layer by DRIE. (d) The structures are released by etching silicon oxide in liquid HF.

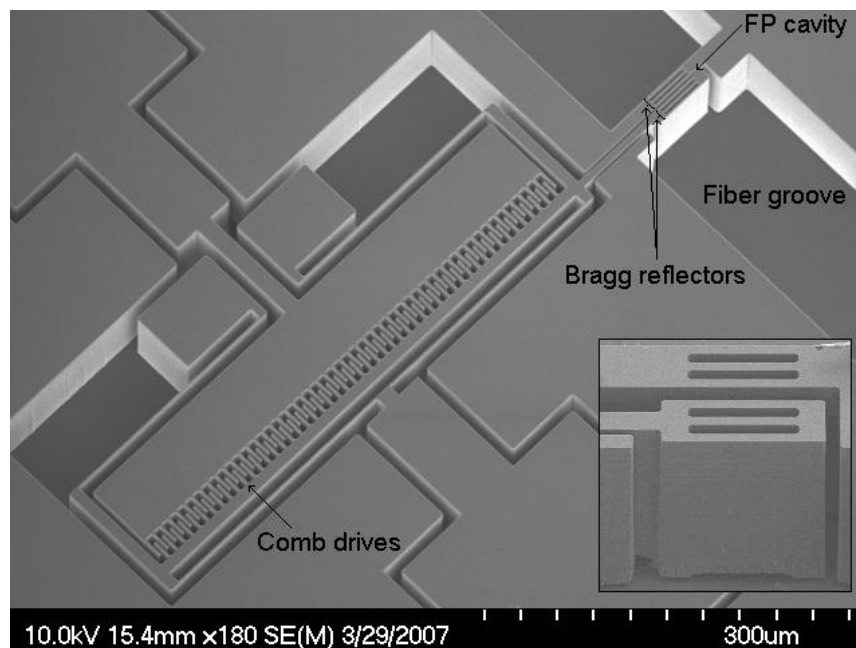


Fig. 4. SEM photograph of one silicon microfabricated Fabry-Pérot device. The inset is a zoom on the two Bragg mirrors composing the FP cavity.

4. RESULTS

In this section we will first report the behavior of the Bragg grating used as one mirror of the FP. Then we will present the FP itself. Finally we will demonstrate the effect of tuning the air gap of the silicon FP cavity.

4.1 Bragg gratings

We experimentally observed the reflection bandwidth decreasing while increasing the order of silicon layers as predicted in the previous section. Figure 5 shows three different experimental reflection spectra for 21st, 41st and 101st order of silicon. We can clearly see that the number of reflection peak increases with higher orders.

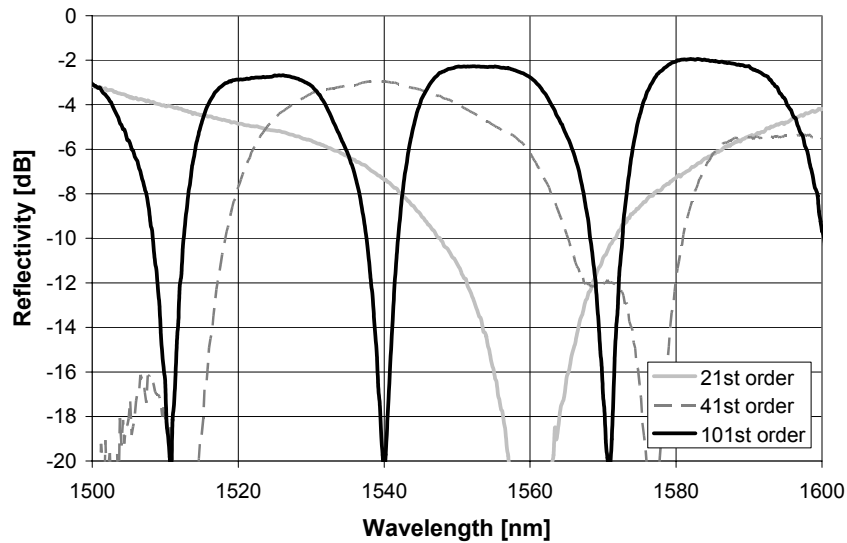


Fig. 5. Experimental spectra of three devices having 21st, 41st and 101st order of silicon

Figure 6 shows the reflection spectra of one fabricated Bragg reflector and of the corresponding simulation. The overall spectral behaviors are very similar. Since reflection losses were not considered in the simulations, the experimental data present higher reflection losses compared to simulations. The reflection losses are mainly due to verticality deviations of the walls and due to scattering. Other imperfections are introduced by the fabrication process. In particular, the silicon walls are thinner than expected because of the DRIE step. The real dimensions of the grating differ from the ideal ones computed by equation 1 and therefore the real spectra differ from the ideal ones shown in figure 1. A deviation on the wall thickness generates a larger bandwidth and causes the reflection and transmission peaks to shift wavelength.

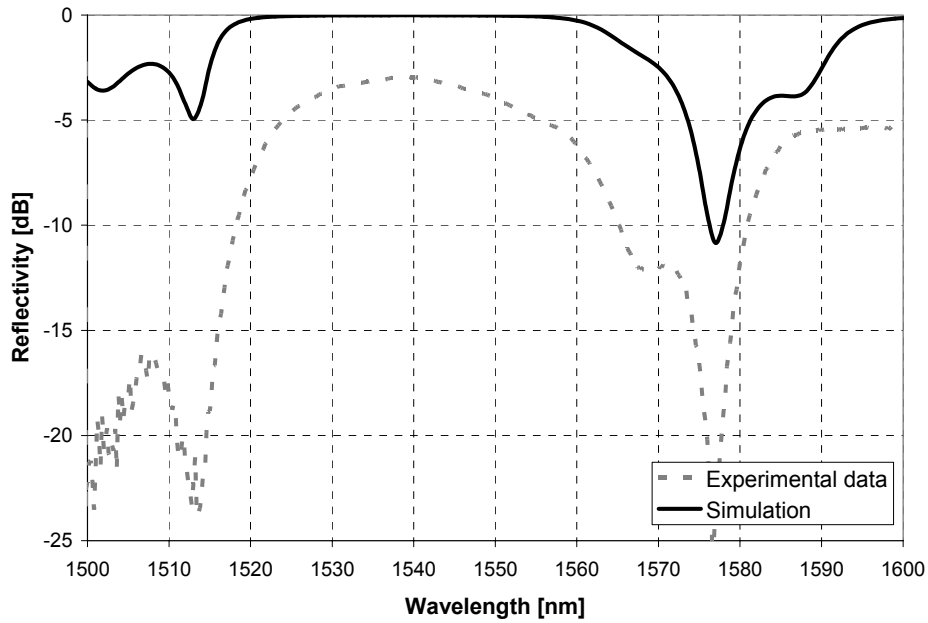


Fig. 6. Simulated (plain line) and measured (dotted line) reflectivity for a Bragg grating with a 41st silicon order, 11th air order and three silicon walls.

4.2 Fabry-Perot

First, we will consider fixed FP filters. The transmission spectrum has a typical band-pass behavior for a FP filter (Fig. 7). The transmission loss is -11dB which is comparable to previously reported silicon filter²⁻³ and the isolation is -20dB. The bandwidth at -3dB is 14 nm.

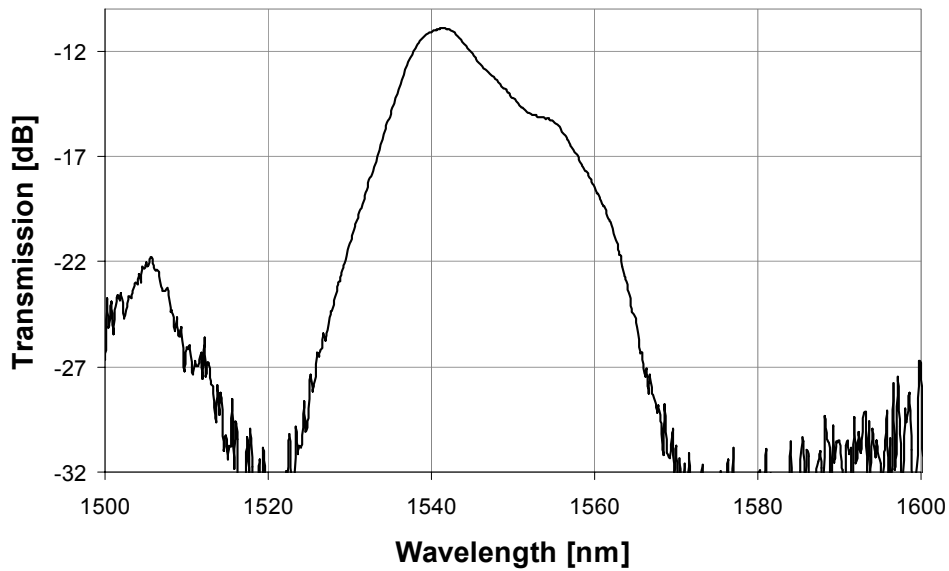


Fig. 7. Experimental transmission spectrum of a fabricated silicon FP cavity.

In a second step, we fabricate tunable FP cavities that are actuated using electrostatic comb drive suspended by four springs (Fig. 8). The comb drive allows a uniform displacement of the grating by applying a low voltage difference between the combs. The uniform modulation of this air gap is of a prime importance and represents a significant improvement compared to Lipson². Indeed, a non-uniform modulation would generate an angle between the two Bragg reflectors changing the resonance properties of the FP. These changes could be expressed by a different filtered wavelength, limited tuning range or by increasing significantly transmission losses. Figure 9 shows the effect on the spectra of the air gap tuning of a FP cavity. The initial transmission peak is 1592nm. As voltage is increased, the air gap between the two Bragg reflectors is decreased. Thus, the transmission peak shifts towards smaller wavelengths. The filter can be tuned continuously down to 1519nm for a total tuning range of 73nm. The FWHM varies from 6 to 10nm. The maximum applied voltage (maximum tuning range of the cavity) is 15.4V.

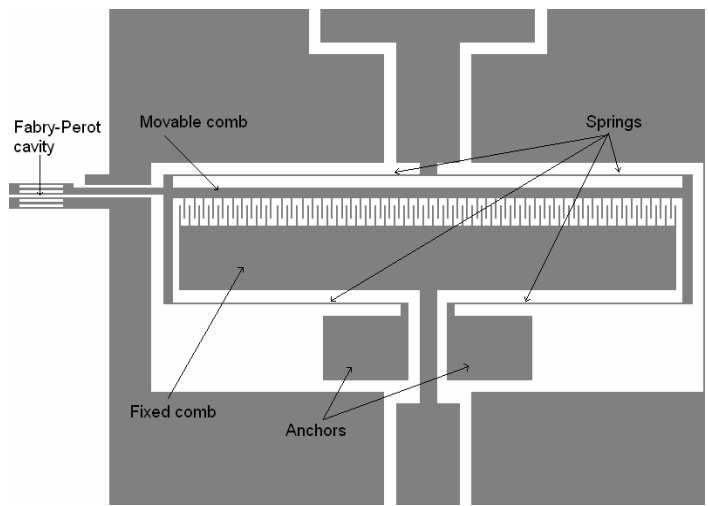


Fig. 8. Schematic of the device including the comb drive actuator and the four springs mechanism.

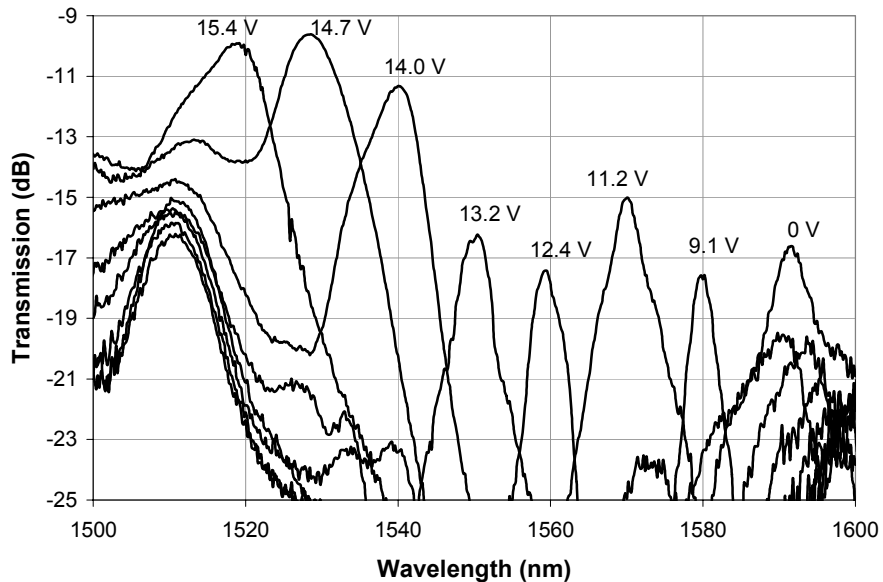


Fig. 9. Transmission spectra of the FP filter tuned from 1592nm down to 1519nm. The voltage applied to the comb drive actuator goes from 0V to 15.4V.

We characterized the modulation of the air gap of the FP filter versus the applied voltage (Fig. 10). The measurements were made by a dynamic white light interferometer. One can see that the maximum tuned wavelength is reached when the air gap is reduced of about 850nm, corresponding to the maximum applied voltage of 15.4V.

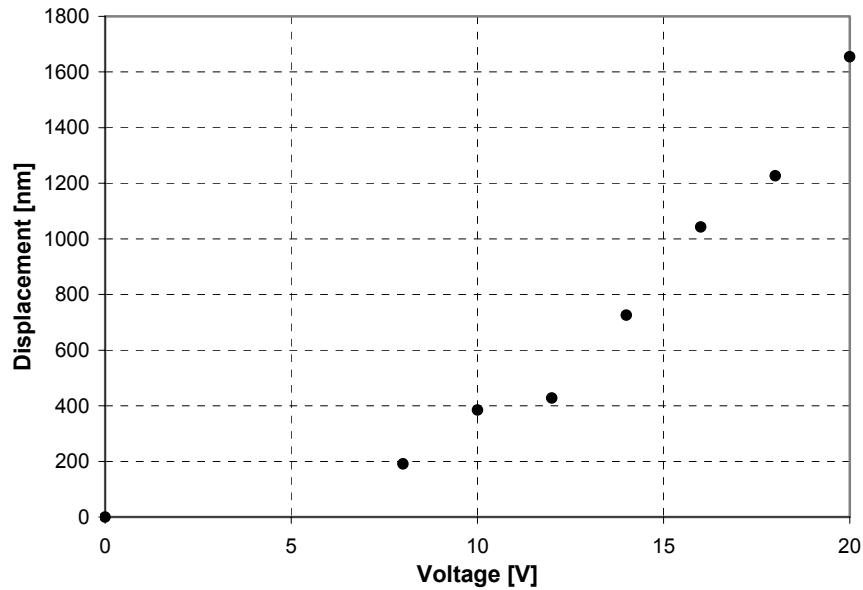


Fig. 10. Measured displacement of the one Bragg mirror versus applied voltage.

5. CONCLUSION

The design of a continuous tunable Fabry-Perot micro machined in silicon is presented. We demonstrate a novel highly tunable FP filter in silicon that is fabricated in one single etch step. Our process allows good wall roughness of 26.2nm rms and high verticality of less than 0.5°. Moreover, the modulation of the air gap is made uniform using a comb drive and a set of four springs. Measured optical characteristics are in good agreement with the predicted ones from the numerical simulations. We demonstrated theoretically and experimentally the influence of the order of the silicon/air pair. The tuning effect of the FP air gap is reported on a bandwidth as large as 73nm covering more than the whole C-band. The transmission losses are -11dB. The maximum actuation voltage required to cover the whole tuning bandwidth is 15.4 V.

6. REFERENCES

- ¹ S.-S. Yun, K.-W. Jo, J.-H. Lee, "Crystalline Si-based in-plane tunable Fabry-Perot filter with wide tunable range," in *IEEE/LEOS International Conference on Optical MEMS and Their Applications*, pp 77-78, 2003.
- ² A. Lipson, E. M. Yeatman, "Free-space MEMS tunable optical filter on (110) silicon", in *International Conference on Optical MEMS and Their Applications*, Oulu, Finland, 2005, pp. 73-74, IEEE/LEOS.
- ³ B. Saadany, M. Malak, F. Marty, Y. Mita, D. Khalil, and T. Bourouina, "Electrostatically-tuned Optical Filter Based on Silicon Bragg Reflectors", in *IEEE/LEOS International Conference on Optical MEMS and Their Applications*, Big Sky, Montana, 2006, pp. 86-87.

- ⁴ M. W. Pruessner, T. H. Stievater, and W. S. Rabinovich, "Integrated waveguide Fabry–Perot microcavities with silicon/air Bragg mirrors", *Optics Letters*, **Vol. 32**, No. 5, 2007.
- ⁵ J. Masson, S. Bergeron, A. Poulin, N. Godbout and Y.-A. Peter, "Tunable erbium doped fiber laser using a silicon micro-electro-mechanical (MEM) Fabry-Perot cavity", accepted in *IEEE/LEOS International Conference on Optical MEMS and Nanophotonics*, Hualien, Taiwan, August 2007.
- ⁶ Y.-A. Peter, F. B. Koné, J. Masson and N. Godbout, "Tunable micro-electromechanical grating in silicon," (invited paper) in *SPIE Optomechatronic Micro/Nano Devices and Components II*, Optics East 2006, Boston, Massachusetts, vol. 6376, paper 04, SPIE.